

## Studies on the Electronic Structures of Hydrocarbon Diradicals by the Unrestricted Hartree-Fock Theory

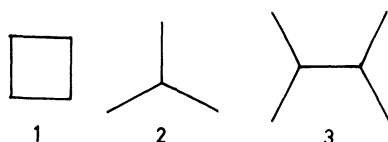
Katsufumi HASHIMOTO\* and Hideo FUKUTOME

Department of Physics, Kyoto University, Sakyo-ku, Kyoto 606

(Received February 16, 1981)

Electronic structures of low-lying states of cyclobutadiene, trimethylenemethane (**2**), and tetramethylenethane (**3**) are studied by the unrestricted Hartree-Fock (UHF) theory. Characteristics of electronic correlations, called dynamical spin polarization effect, in these molecules are well described by corresponding orbitals and spin density structures of low-lying UHF solutions. The spin polarization of  $\sigma$  electrons is found to be relatively small but not negligible for quantitative discussion. The two low-lying singlet states of **2** are described by two UHF solutions with different spin density structures. The fact that the singlet UHF state of **3** lies a little below the triplet UHF state is explained by the difference in the spin polarization of the bonding  $\pi$  electrons between the singlet and triplet states. Two rules are given which predict the spin structure of low-lying UHF states and the spin multiplicity of ground states of hydrocarbon diradicals. These rules are applied to 1,1,2,3,3-pentamethylene-propane and 1,3-dimethylenecyclobutadiene, which confirms their validity.

Recent theoretical studies on cyclobutadiene (**1**) and trimethylenemethane (**2**) have revealed the importance



of correlation effects in determining the spin multiplicity of ground states and the stable geometry of low-lying states of hydrocarbon diradicals. Borden<sup>1)</sup> showed that a strong correlation effect in **1** causes a violation of Hunt's rule and makes the ground state singlet. This effect was also shown to make the equilibrium geometry close to a square. These results are in agreement with experiments.<sup>2)</sup> As for **2**, Yacony and Schaefer III<sup>3a)</sup> and Borden<sup>3b)</sup> pointed out that the correlation of the two nonbonding (NB) electrons much reduces the energy difference in the singlet state between the planar geometry and the geometry with a methylene group orthogonal to the remaining allyl group.

These results indicate that in order to understand electronic properties of hydrocarbon diradicals, it is necessary to clarify correlation effects involved. As pointed out by Borden<sup>1)</sup> and Kollmar and Staemmler,<sup>4)</sup> the most important correlation effect in diradicals is similar to the spin polarization effect in free radicals. They called it the dynamical spin polarization effect. Therefore, the unrestricted Hartree-Fock (UHF) theory is powerful in analyzing the correlation effect. In this paper, we apply the UHF theory to three diradicals **1**, **2**, and tetramethylenethane (**3**). We show that the corresponding orbitals and the spin density structure in the UHF theory well describe the dynamical spin polarization effect in low-lying states of the molecules. Concerning **3**, the singlet state is predicted to lie a little below the triplet state. From results for **1**, **2**, and **3**, we derive simple rules to predict the spin multiplicity of ground states and the spin structure of low-lying UHF solutions of hydrocarbon diradicals.

UHF calculations were made with the INDO approximation<sup>5)</sup> using the computer program written by Takahashi and Igawa which uses the direct optimization

method developed by Igawa and Fukutome<sup>6)</sup> and is capable of calculating UHF solutions and their instabilities of any types. We use the notation proposed by Fukutome<sup>7)</sup> for the types of UHF solutions and their instabilities.

### Analysis of a Simplified Model of Diradicals with Two Electrons in Two NB MOs

Before performing all-valence-electron UHF analyses, we examine in this section UHF solutions for a simple model with two degenerate NB MOs  $\phi_A$  and  $\phi_B$  of different symmetries in a spatial symmetry group. In the model, there are one triplet state ( $\Psi_T$ ) and three singlet states ( $\Psi_{S1}$ ,  $\Psi_{S2}$ , and  $\Psi_{S3}$ ) which are represented as

$$\begin{aligned}\Psi_T &= (\phi_A\phi_B - \phi_B\phi_A)/\sqrt{2} \Theta_T, \\ \Psi_{S1} &= (\phi_A\phi_A - \phi_B\phi_B)/\sqrt{2} \Theta_S, \\ \Psi_{S2} &= (\phi_A\phi_A + \phi_B\phi_B)/\sqrt{2} \Theta_S, \\ \Psi_{S3} &= (\phi_A\phi_B + \phi_B\phi_A)/\sqrt{2} \Theta_S, \\ \Theta_T &= (\alpha\beta + \beta\alpha)/\sqrt{2}, \quad \Theta_S = (\alpha\beta - \beta\alpha)/\sqrt{2}.\end{aligned}$$

Their energies are given by

$$\begin{aligned}E_T &= 2K + \langle AA|BB \rangle - \langle AB|BA \rangle, \\ E_{S1} &= 2K + \gamma - \langle AB|BA \rangle, \\ E_{S2} &= 2K + \gamma + \langle AB|BA \rangle, \\ E_{S3} &= 2K + \langle AA|BB \rangle + \langle AB|BA \rangle,\end{aligned}$$

where

$$\langle AB|A'B' \rangle = e^2 \int d1 d2 \phi_A(1) \phi_B(1) \phi_{A'}(2) \phi_{B'}(2) / r_{12},$$

and we assume that the single particle energies of  $\phi_A$  and  $\phi_B$  are equal to  $K$  and that  $\langle AA|AA \rangle = \langle BB|BB \rangle = \gamma$ . By the relation

$$\gamma > \langle AA|BB \rangle > \langle AB|BA \rangle > 0$$

the energetic order of the states except  $\Psi_{S3}$  is determined as

$$E_{S2} > E_{RHF} > E_{S1} > E_T,$$

where RHF means the restricted HF state  $|\phi_A\alpha, \phi_A\beta\rangle$  with the energy  $E_{RHF} = 2K + \gamma$ . The energetic position of  $\Psi_{S3}$  depends on the extent of the differential overlap

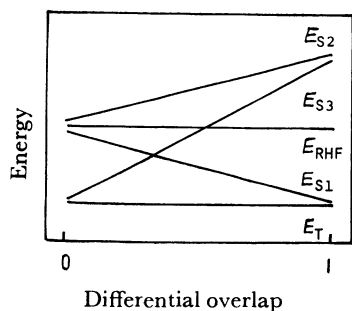


Fig. 1. The correlation diagram of low-lying states of diradicals against the extent of the differential overlap between the two NB MOs.

between  $\phi_A$  and  $\phi_B$ . Let's consider two extreme cases. When the overlap is nearly complete,  $\langle AA|BB \rangle$  is nearly equal to  $\gamma$ , so that  $\Psi_{S3}$  is higher than the RHF and nearly degenerate with  $\Psi_{S2}$ .  $\Psi_{S1}$  and  $\Psi_T$  also are nearly degenerate. When  $\phi_A$  and  $\phi_B$  are disjoint,  $\langle AA|BB \rangle$  is much smaller than  $\gamma$ , so that  $\Psi_{S3}$  is lower than the RHF and nearly degenerate with  $\Psi_T$ .  $\Psi_{S1}$ ,  $\Psi_{S2}$ , and the RHF are also nearly degenerate. By connecting these extreme cases we obtain dependence of the energetic order of the four states on the overlap of  $\phi_A$  and  $\phi_B$  as shown in Fig. 1. It is found that in the two-electron model the ground state is always the triplet state. In the two extreme cases, however, the singlet state lies close to the triplet state, so that the energetic order is possible to change in the all-valence-electron model. Figure 1 shows that in the case of the intermediate overlap the two singlet states  $\Psi_{S1}$  and  $\Psi_{S3}$  may lie below the RHF. In the following, we examine how the two singlet states are described by the UHF theory.

First we obtain the UHF solution emerging from the instability of the RHF. The four instability matrices ( ${}^1ST_{\pm}$ ,  ${}^3ST_{\pm}$ )<sup>7</sup> of the RHF are  $1 \times 1$  dimensional in the model and are given by

$${}^1ST_{+} = 2(a-b), \quad {}^1ST_{-} = {}^3ST_{+} = -2b,$$

$${}^3ST_{-} = -2(a+b),$$

$$a = \langle AB|BA \rangle, \quad b = (\gamma - \langle AA|BB \rangle)/2, \quad a, b > 0.$$

Because the  ${}^3ST_{-}$  instability matrix has the lowest negative eigenvalue, we consider this instability. The  ${}^3ST_{-}$  instability of the RHF indicates that there is an axial spin density wave (ASDW) UHF solution (ASDW1) lower in energy than the RHF. The orbitals of ASDW1, which is a real DODS solution, are a spin polarized mixture of  $\phi_A$  and  $\phi_B$

$$\text{ASDW1} = |\phi_{1+}\alpha, \phi_{1-}\beta|, \quad \phi_{1\pm} = \cos\theta\phi_A \pm \sin\theta\phi_B,$$

and the energy is given by

$$E_{\text{ASDW1}} = E_{\text{RHF}} - (a+b) \sin^2 2\theta.$$

$E_{\text{ASDW1}}$  has a minimum at  $\theta=45^\circ$ , so that we obtain

$$\phi_{1\pm} = (\phi_A \pm \phi_B)/\sqrt{2},$$

$$E_{\text{ASDW1}} = 2K + (\gamma + \langle AA|BB \rangle)/2 - \langle AB|BA \rangle.$$

The wave function of ASDW1 is expanded as

$$(\Psi_{S1} - \Psi_T)/\sqrt{2},$$

showing that the singlet component of ASDW1 is  $\Psi_{S1}$ .

Next we examine the stability of ASDW1. The four instability matrices ( $A_{\pm}M_{\pm}$ )<sup>7</sup> of ASDW1 are  $2 \times 2$

dimensional in the model and are given by

$$A_{+}M_{+} = \begin{pmatrix} 2a & 2b \\ 2b & 2a \end{pmatrix}, \quad A_{+}M_{-} = \begin{pmatrix} 2a & 0 \\ 0 & 2a \end{pmatrix},$$

$$A_{-}M_{\pm} = \begin{pmatrix} -b & -b \\ -b & -b \end{pmatrix}.$$

The lowest eigenvalue of the  $A_{+}M_{+}$  instability matrix is  $2(a-b)$  with the eigenvector  $\begin{pmatrix} 1 \\ -1 \end{pmatrix}$ . Therefore, if  $a-b < 0$  which is the same condition as  $E_{S3} < E_{S1}$ , ASDW1 is  $A_{+}M_{+}$  unstable, that is, ASDW1 is unstable for a spin unflip excitation and there is another ASDW solution (ASDW2) lower in energy than ASDW1. ASDW2's orbitals are determined by the eigenvector  $\begin{pmatrix} 1 \\ -1 \end{pmatrix}$  of the  $A_{+}M_{+}$  instability in the following form

$$\text{ASDW2} = |\phi'_{1+}\alpha, \phi'_{1-}\beta|, \quad \phi'_{1\pm} = \cos\theta\phi_{1\pm} \pm \sin\theta\phi_{2\pm},$$

$$\phi_{2+} = \phi_{1-} = (\phi_A - \phi_B)/\sqrt{2},$$

$$\phi_{2-} = \phi_{1+} = (\phi_A + \phi_B)/\sqrt{2},$$

and the energy is given by

$$E_{\text{ASDW2}} = E_{\text{ASDW1}} + (a-b) \sin^2 2\theta.$$

$E_{\text{ASDW2}}$  has a minimum at  $\theta=45^\circ$ , so that we obtain

$$\phi'_{1+} = \phi_A, \quad \phi'_{1-} = -\phi_B, \quad E_{\text{ASDW2}} = 2K + \langle AA|BB \rangle.$$

Clearly the singlet component of ASDW2 is  $\Psi_{S3}$ .

Last we examine the stability of ASDW2. The instability matrices of ASDW2 are

$$A_{+}M_{+} = \begin{pmatrix} 2b & 2a \\ 2a & 2b \end{pmatrix}, \quad A_{+}M_{-} = \begin{pmatrix} 2b & 0 \\ 0 & 2b \end{pmatrix},$$

$$A_{-}M_{\pm} = \begin{pmatrix} -a & -a \\ -a & -a \end{pmatrix}.$$

Therefore, if  $b-a < 0$  which is the same condition as  $E_{S1} < E_{S3}$ , ASDW2 is  $A_{+}M_{+}$  unstable. We can show similarly that the UHF solution arising from this instability is ASDW1.

The above results show that ASDW1 and ASDW2 well describe the two low-lying singlet states ( $\Psi_{S1}$  and  $\Psi_{S3}$ ) which involve strong electronic correlations. The stability relations among the three HF solutions, the RHF, ASDW1, and ASDW2, are summarized in Table 1. We note that in the two-electron model, if  $E_{S1} > (<) E_{S3}$ , ASDW1 (ASDW2) is always unstable, but that this is not necessarily the case with all-valence-electron calculations. This situation is also shown by the second scheme in Table 1.

TABLE 1. POSSIBLE INSTABILITY RELATIONS AMONG THE THREE HF SOLUTIONS OF DIRADICALS

	${}^3ST_{-}$	$A_{+}M_{+}$
$E_{\text{RHF}} > E_{S1} > E_{S3}$ , RHF	$\longrightarrow$ ASDW1	$\longrightarrow$ ASDW2
$(E_{\text{RHF}} > E_{S1} \approx E_{S3})$ , RHF	$\xrightarrow{{}^3ST_{-}}$ ASDW1,	ASDW2)
$E_{\text{RHF}} > E_{S3} > E_{S1}$ , RHF	$\xrightarrow{{}^3ST_{-}}$ ASDW1	$\xleftarrow{A_{+}M_{+}}$ ASDW2
$E_{S3} > E_{\text{RHF}} > E_{S1}$ , RHF	$\xrightarrow{{}^3ST_{-}}$ ASDW1	

### UHF Calculation on Cyclobutadiene

We performed an all-valence-electron UHF calculation on **1** by varying the C-C bond length ( $R$ ) from

1.61 Å to 1.31 Å. The other geometrical parameters are fixed as shown in Fig. 2a. In the geometries the RHF  $\pi$  orbitals are a bonding (B)  $\pi$  MO ( $\phi_1$ ), two nearly degenerate NB  $\pi$  MOs ( $\phi_2$ ,  $\phi_3$ ), and an antibonding (AB)  $\pi$  MO ( $\phi_4$ ):

$$\phi_1 = (\chi_1 + \chi_2 + \chi_3 + \chi_4)/2, \quad \phi_2 = (\chi_1 + \chi_2 - \chi_3 - \chi_4)/2,$$

$$\phi_3 = (\chi_1 - \chi_2 + \chi_3 - \chi_4)/2, \quad \phi_4 = (\chi_1 - \chi_2 - \chi_3 + \chi_4)/2,$$

where  $\chi_i$  is the  $\pi$  atomic orbital (AO) of the  $i$ -th carbon atom in Fig. 2a. The MOs  $\phi_1$ – $\phi_4$  are of  $b_{1u}$ ,  $b_{2g}$ ,  $b_{3g}$ ,

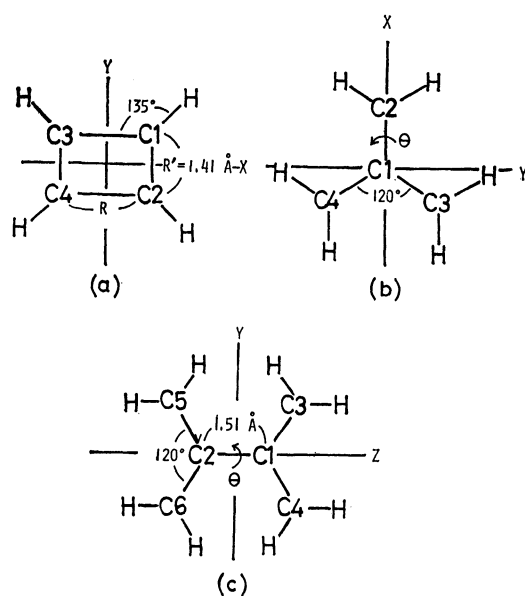


Fig. 2. Geometries used in the calculations for **1**, **2**, and **3**. All the C-H bond lengths are fixed to 1.1 Å, the C-C bond lengths, whose values are not indicated, to 1.41 Å, and all the H-C-H angles to 120°. **1** has the  $D_{2h}$  and  $D_{4h}$  symmetries at  $R \neq R'$  and  $R = R'$ , respectively. **2** has the  $D_{3h}$ ,  $C_{2v}$ , and  $C_2$  symmetries at  $\theta = 0^\circ$ ,  $90^\circ$ , and  $\theta \neq 0^\circ$  and  $90^\circ$ , respectively, and **3** has the  $D_{2h}$ ,  $D_{2d}$ , and  $D_2$  symmetries at  $\theta = 0^\circ$ ,  $90^\circ$ , and  $\theta \neq 0^\circ$  and  $90^\circ$ , respectively.

and  $a_u$  symmetries in the  $D_{2h}$  point group, respectively. As  $R$  is varied, the MOs  $\phi_2$  and  $\phi_3$  cross at square geometries, so that there are two RHF ground states with different occupancies of the  $\pi$  MOs: RHF1 =  $(\phi_1)^2(\phi_2)^2$  and RHF2 =  $(\phi_1)^2(\phi_3)^2$ . RHF1 and RHF2 are the RHF ground states in the regions  $R > R'$  and  $R < R'$ , respectively. Near the square geometry they become  $^3ST^-$  unstable. Because the differential overlap between the two NB MOs is complete, this case corresponds to the last scheme of Table 1 and an ASDW solution, ASDW1, emerges from the instability. ASDW1 connects smoothly RHF1 and RHF2. The correlation diagram of the  $\pi$  MOs and the adiabatic potentials of the RHF and the UHF solutions are shown in Fig. 3. This shows that ASDW1 is the HF ground state near the square geometry and that the triplet ASDW solution is higher in energy than ASDW1 in contrast to the two-electron model. The equilibrium geometry of the singlet ground state obtained from ASDW1's potential becomes very close to the square one in contrast to the rectangular equilibrium geometries of the RHF's potentials. These

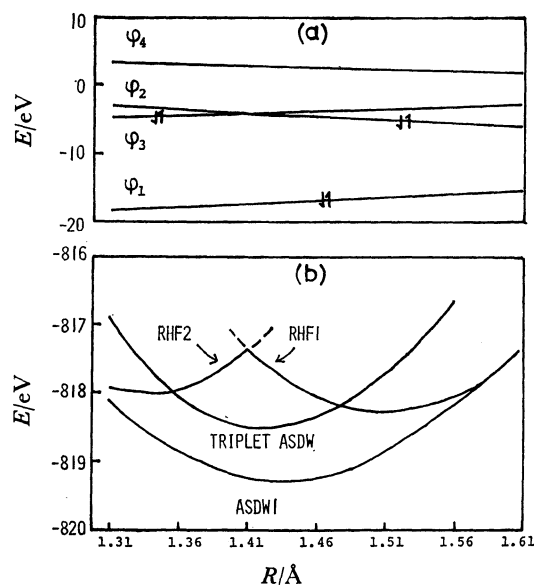


Fig. 3. The correlation diagram of the Hückel type  $\pi$  MOs (a), and the adiabatic potentials of the RHF, ASDW1 and the triplet ASDW (b) of cyclobutadiene.

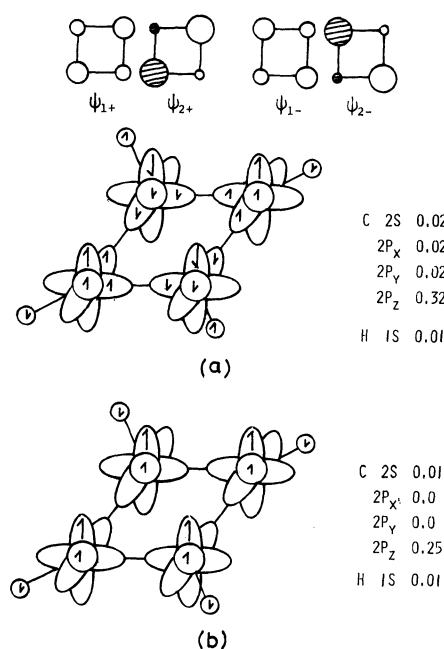


Fig. 4. The  $\pi$  corresponding orbitals and the spin density structure of ASDW1 (a) and the spin density structure of the triplet ASDW (b) of cyclobutadiene. The carbon  $\pi$  AOs with positive MO coefficients are represented by white circles and those with negative MO coefficients by shaded ones. The radii of the circles are proportional to the magnitudes of the MO coefficients. The spin densities with positive and negative  $z$  components are represented by up- and downward arrows, respectively. The magnitudes of the spin densities on carbon and hydrogen AOs are the same for all the C-H units except their signs.

features stem from the correlation effect which becomes important as the square geometry is neared.

In order to analyze the electronic correlation in

ASDW1, we show in Fig. 4 the  $\pi$  corresponding orbitals and the spin density structure of ASDW1 at the equilibrium geometry. The spin density structure of the triplet ASDW is also shown for comparison. The excitations contributing to the  $^3\text{ST}_-$  instability which produces ASDW1 from the RHF have the  $B_{1g}$  symmetry. Therefore, the  $\pi$  excitations  $\phi_2 \rightarrow \phi_3$  (or  $\phi_3 \rightarrow \phi_2$ ) and  $\phi_1 \rightarrow \phi_4$  contribute to the instability. Consequently, not only the NB  $\pi$  orbitals but also the B  $\pi$  orbitals are spin polarized as follows:

$$\phi_{1\pm} = \cos \theta_1 \phi_1 \pm \sin \theta_1 \phi_4, \quad \phi_{2\pm} = \cos \theta_2 \phi_2 \pm \sin \theta_2 \phi_3.$$

The  $\sigma$  orbitals are also spin polarized, but to a smaller extent than the  $\pi$  orbitals, due to the  $\sigma$  excitation with the  $B_{1g}$  symmetry.

The triplet ASDW is obtained with the trial wave function

$$\Psi_T^0 = |\text{core}, \phi_1\alpha, \phi_1\beta, \phi_2\alpha, \phi_3\alpha|,$$

where core represents the doubly occupied RHF  $\sigma$  MOs. After the SCF procedure, the  $\pi$  orbitals remain unchanged but the core part is spin polarized with the corresponding orbitals retaining the same symmetries as the original RHF  $\sigma$  orbitals.

The spin polarization of the B  $\pi$  orbital  $\phi_1$  appears only in the singlet state. Its physical significance is as follows.<sup>1)</sup> The splitting of the B  $\pi$  orbital occurs in such a way that  $\phi_{1\pm}$  overlaps  $\phi_{2\pm}$  more than  $\phi_{2\mp}$  as shown in Fig. 4. Such coherent splittings of  $\phi_{1\pm}$  and  $\phi_{2\pm}$  reduce the Coulomb repulsion between the electrons of opposite spins because they are localized to different regions. The electrons of the same spin localize to the same region but this does not enhance the Coulomb repulsion between them because the Pauli principle prevents their close encounter. In contrast to the singlet state, the spin polarization of the B  $\pi$  electrons is not induced in the triplet state because the spin density of the NB  $\pi$  electrons is uniform in the triplet state. The spin polarization of the B  $\pi$  electrons which operates only in the singlet state makes the singlet ASDW lower in energy than the triplet ASDW.

Next we discuss on the spin polarization of the  $\sigma$  electrons shown in Fig. 4. The spin polarization of the  $\sigma$  electrons is induced in such a way that the  $\sigma$  spin densities on a carbon atom and that on adjacent hydrogen atom are arranged in the same and opposite directions, respectively, compared to that of the  $\pi$  spin density on the carbon atom. This enhances the exchange interaction between the  $\sigma$  electrons and the  $\pi$  electrons on each carbon atom and reduces the Coulomb repulsion between  $\sigma$  electrons. The magnitude of the  $\sigma$  spin polarization is relatively small. However, its effects are not so small as can be neglected in quantitative discussion.

### UHF Calculation on Trimethylenemethane

We performed a UHF calculation on **2** by rotating a methylene group out of the plane of the remaining allyl group. The other geometrical parameters are fixed as shown in Fig. 2b. At the planar geometry, the RHF  $\pi$  MOs are a B  $\pi$  MO ( $\phi_1$ ), two degenerate NB  $\pi$  MOs ( $\phi_2, \phi_3$ ), and an AB  $\pi$  MO ( $\phi_4$ ):

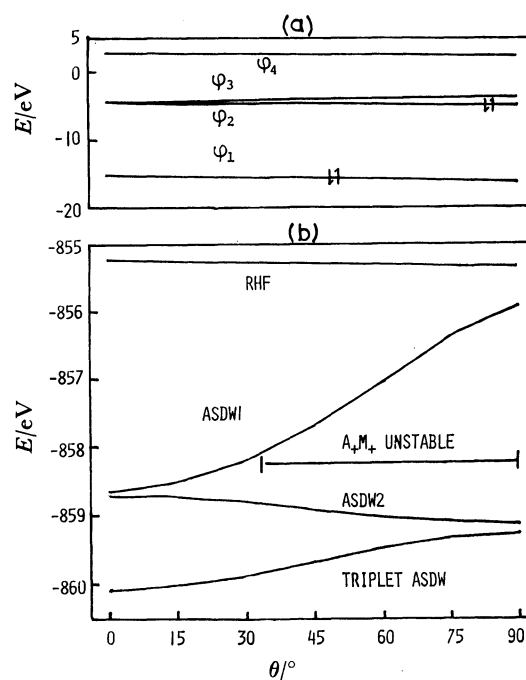


Fig. 5. The correlation diagram of the Hückel type MOs (a) and the adiabatic potentials of the RHF, ASDWs, and the triplet ASDW (b) of trimethylenemethane. The  $A_1M_+$  instability domain of ASDW1 is also indicated. The region out of the domain corresponds to the second scheme in Table 1.

$$\begin{aligned} \phi_1 &= a\chi_1 + b(\chi_2 + \chi_3 + \chi_4)/\sqrt{3}, \quad \phi_2 = (\chi_3 - \chi_4)/\sqrt{2}, \\ \phi_3 &= (2\chi_2 - \chi_3 - \chi_4)/\sqrt{6}, \\ \phi_4 &= -b\chi_1 + a(\chi_2 + \chi_3 + \chi_4)/\sqrt{3}, \quad a \approx b \approx 0.7. \end{aligned}$$

The MOs  $\phi_1$  and  $\phi_4$  belong to the  $a_2''$  (b) symmetry and  $\phi_2$  and  $\phi_3$  to the  $e''$  (a and b) symmetry at the planar  $D_{3h}$  geometry (nonplanar  $C_2$  geometry). In the process of the internal rotation, the two NB MOs remain nearly degenerate ( $\phi_2$  lies a little below  $\phi_3$ ) as shown in Fig. 5a. The LCAO expression of  $\phi_2$  is unchanged while the main AO component of  $\phi_3$  turns out to be the p probe perpendicular to the twisted methylene group. Therefore, in the rotation the differential overlap between the two NB MOs varies from medium to nearly zero. This situation corresponds to the left half side of Fig. 1 and the first and second schemes of Table 1. Therefore, two singlet UHF states exist below the RHF. The UHF adiabatic potentials are shown in Fig. 5b. This calculation shows that the ground state is triplet and that its equilibrium geometry is planar. On the other hand, the lowest singlet UHF state (ASDW2) has the orthogonal equilibrium geometry. These results are in agreement with other calculations<sup>3)</sup> and experiments.<sup>9)</sup> It should be noted that at the planar geometry the two singlet states which are approximated by ASDW1 and ASDW2 are degenerate and belong to the  $E'$  representation of the  $D_{3h}$  point group. The calculated energies of ASDW1 and ASDW2 at the planar geometry are not exactly the same. However, the gap is very small and much reduced compared to the value in the RHF calculation of the two state.<sup>3c)</sup>

In order to analyze the electronic correlation among

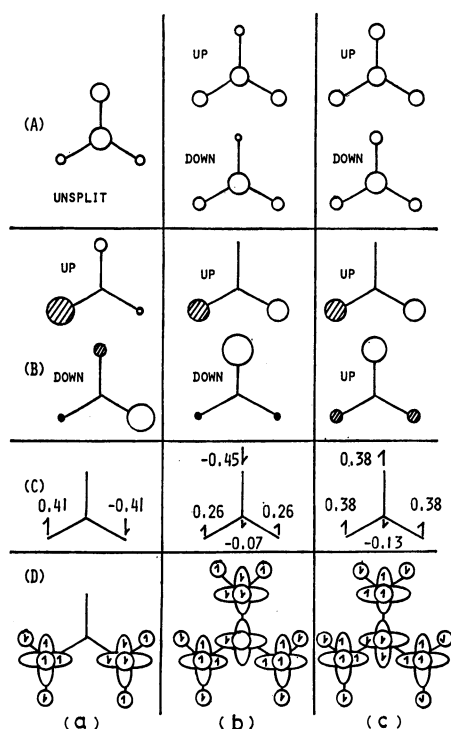


Fig. 6. The corresponding orbitals for the B  $\pi$  electrons (A) and for the NB  $\pi$  electrons (B), and the spin density structure on the  $\pi$  AOs (C) and on the  $\sigma$  AOs (D) of ASDW1 (a), ASDW2 (b), and the triplet ASDW (c) of planar trimethylenemethane. The numerals in (C) are the magnitudes of the spin densities. Those on the  $\sigma$  AOs are either  $\pm 0.01$  or  $\pm 0.02$ .

the three UHF states, we show in Fig. 6 the  $\pi$  corresponding orbitals and the spin density structures of the UHF states at the planar geometry. The  $^3\text{ST}^-$  instability which connects the RHF with ASDW1 has the B symmetry in the  $C_2$  group. We adopted the  $C_2$  symmetry because the RHF with the occupancy  $(\phi_1)^2(\phi_2)^2$  of the  $\pi$  MOs is of symmetry adapted only to the  $C_2$  group. The excitations  $\phi_2 \rightarrow \phi_3$  and  $\phi_2 \rightarrow \phi_4$  with the B symmetry contribute to the instability. Consequently, the NB orbitals in ASDW1 are spin polarized in the following manner:

$$\psi_{2\pm} = \cos \theta_1 \phi_2 \pm \sin \theta_1 (\cos \theta_2 \phi_3 - \sin \theta_2 \phi_4).$$

After the SCF procedure,  $\phi_1$  also is mixed into  $\psi_{2\pm}$  because it has the same symmetry as  $\phi_3$  and  $\phi_4$  in the  $C_2$  group.

ASDW2's orbitals are adapted to the  $C_2$  symmetry and not to the  $D_{3h}$  one because its trial wave function

$$|\text{core}, \phi_1\alpha, \phi_1\beta, \phi_2\alpha, \phi_3\beta|$$

has the  $C_2$  symmetry and not the  $D_{3h}$  one. Therefore,  $\phi_1$ ,  $\phi_3$ , and  $\phi_4$  with the same b symmetry are mixed in ASDW2 after the SCF procedure, but  $\phi_2$  is unchanged:

$$\psi'_{2-} = \cos \theta_3 \phi_3 + \sin \theta_3 (\cos \theta_4 \phi_4 + \sin \theta_4 \phi_1),$$

$$\psi'_{1-} = \cos \theta_5 \phi_1 - \sin \theta_5 (\cos \theta_6 \phi_4 - \sin \theta_6 \phi_3),$$

$$\psi'_{1+} = \cos \theta_5 \phi_1 - \sin \theta_5 (\cos \theta_6 \phi_3 - \sin \theta_6 \phi_4).$$

The ASDW2's orbitals  $\psi'_{1-}$  and  $\psi'_{2-}$  have large MO weights on  $\chi_1$  and  $\chi_2$  AOs and  $\psi'_{1+}$  does on  $\chi_3$  and  $\chi_4$

AOs so that electrons with different spins are caused to localize in different regions.

The triplet ASDW's orbitals are adapted to the  $D_{3h}$  symmetry because of the  $D_{3h}$  adaptation for the trial wave function

$$|\text{core}, \phi_1\alpha, \phi_1\beta, \phi_2\alpha, \phi_3\alpha|.$$

Therefore, only  $\phi_1$  and  $\phi_4$  with the same  $a_2''$  symmetry are mixed in the triplet ASDW

$$\psi_{1\pm}^t = \cos \theta_{7\pm} \phi_1 \pm \sin \theta_{7\pm} \phi_4.$$

By the spin polarization of  $\psi_{1\pm}^t$  a negative spin density appears on the central carbon atom.

We note that the spin structures of ASDW2 and the triplet ASDW are similar to those of the singlet and triplet GVB wave functions obtained by Davis and Goddard III.<sup>3d)</sup> The forms of the orbitals of ASDW1 and ASDW2 are retained in the process of the rotation because the system has the  $C_2$  symmetry throughout the process. The change in the spin polarization effect in the triplet ASDW also is small.

Next, we clarify the difference between ASDW1 and ASDW2. As mentioned above, ASDW2 is adapted to the  $C_2$  symmetry, so that its spin structure is also invariant to the  $C_2$  spatial rotation. The spin structure of ASDW1 is invariant not to the  $C_2$  rotation but to the joint  $C_2$  rotation of space and spin. This difference between the symmetries of the spin structures means that the singlet components of ASDW1 and ASDW2 belong to different  $C_2$  symmetries as shown by Ozaki.<sup>9)</sup> In fact, the singlet component of ASDW1 has the A symmetry but that of ASDW2 the B symmetry.

### UHF Calculation on Tetramethylenethane

We performed a UHF calculation on **3** by rotating the two allyl groups around the central C-C bond. The other geometrical parameters are fixed as shown in Fig. 2c. At the planar geometry the RHF  $\pi$  MOs are two B  $\pi$  MOs ( $\phi_1, \phi_2$ ), two nearly degenerate NB  $\pi$  MOs ( $\phi_3, \phi_4$ ), and two AB  $\pi$  MOs ( $\phi_5, \phi_6$ ):

$$\phi_1 = a(\chi_1 + \chi_2)/\sqrt{2} + b(\chi_3 + \chi_4 + \chi_5 + \chi_6)/2,$$

$$\phi_2 = a'(\chi_1 - \chi_2)/\sqrt{2} + b'(\chi_3 + \chi_4 - \chi_5 - \chi_6)/2,$$

$$\phi_3 = (\chi_3 - \chi_4 + \chi_5 - \chi_6)/2, \quad \phi_4 = (\chi_3 - \chi_4 - \chi_5 + \chi_6)/2,$$

$$\phi_5 = -b(\chi_1 + \chi_2)/\sqrt{2} + a(\chi_3 + \chi_4 + \chi_5 + \chi_6)/2,$$

$$\phi_6 = -b'(\chi_1 - \chi_2)/\sqrt{2} + a'(\chi_3 + \chi_4 - \chi_5 - \chi_6)/2,$$

$$a \approx b' \approx 0.8, \quad b \approx a' \approx 0.6.$$

The MOs  $\phi_1$ – $\phi_6$  are of  $b_{3u}$ ,  $b_{2g}$ ,  $b_{1g}$ ,  $a_u$ ,  $b_{3u}$ , and  $b_{2g}$  symmetry in the  $D_{2h}$  group, respectively. In the process of the rotation, the two NB MOs remain nearly degenerate and cross at about  $\theta = 40^\circ$  as shown in Fig. 7a. The crossing occurs due to the spiroconjugation effect.<sup>10)</sup> Therefore, there are two RHF ground states with the occupancies  $\text{RHF1} = (\phi_1)^2(\phi_2)^2(\phi_3)^2$  and  $\text{RHF2} = (\phi_1)^2(\phi_2)^2(\phi_4)^2$ . RHF1 and RHF2 are the RHF ground states in the regions  $\theta < 40^\circ$  and  $\theta > 40^\circ$ , respectively. The differential overlap between the two NB MOs is nearly complete throughout the rotation process, so that this case belongs to the last scheme of Table 1 and there is only a singlet ASDW state (ASDW1) below the RHF. The adiabatic potentials of the RHF and

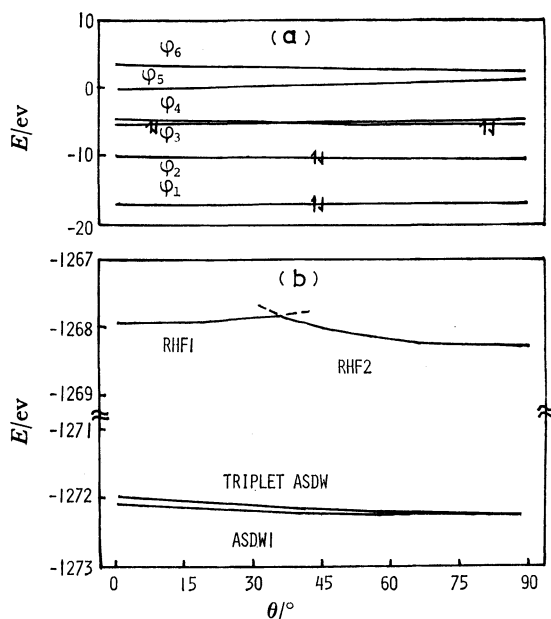


Fig. 7. The correlation diagram of the Hückel type MOs (a) and the adiabatic potentials of the RHF's, ASDW1 and the triplet ASDW (b) of tetramethylethane.

UHF states are shown in Fig. 7b. Our calculation, like a previous one,<sup>10)</sup> shows a rather small energy change in the rotation. The singlet ASDW1 is found to lie a little below the triplet ASDW everywhere and has a very shallow potential minimum at about  $\theta = 50^\circ$ .

Next we examine the electronic correlation between the singlet and triplet ASDW states at the planar geometry. The  $^3\text{ST}_-$  instability which connects the RHF and ASDW1 has the  $B_{1u}$  symmetry. Therefore, the excitations  $\phi_3 \rightarrow \phi_4$ ,  $\phi_2 \rightarrow \phi_5$ , and  $\phi_1 \rightarrow \phi_6$  with the  $B_{1u}$  symmetry contribute to the instability. Consequently, all the orbital pairs are spin polarized as

$$\begin{aligned}\psi_{1\pm}^s &= \cos \theta_1 \phi_1 \pm \sin \theta_1 \phi_6, \quad \psi_{2\pm}^s = \cos \theta_2 \phi_2 \pm \sin \theta_2 \phi_5, \\ \psi_{3\pm}^s &= \cos \theta_3 \phi_3 \pm \sin \theta_3 \phi_4.\end{aligned}$$

The triplet ASDW's orbitals are adapted to the  $D_{2h}$  symmetry because its trial wave function

$$|\text{core}, \phi_1\alpha, \phi_1\beta, \phi_2\alpha, \phi_2\beta, \phi_3\alpha, \phi_4\alpha|$$

has the  $B_{1u}$  symmetry in the  $D_{2h}$  group. After the SCF procedure,  $\phi_2$  and  $\phi_6$  with the  $b_{2g}$  symmetry and  $\phi_1$  and  $\phi_5$  with the  $b_{3u}$  one are mixed in the triplet ASDW to yield

$$\psi_{1\pm}^t = \cos \theta_{4\pm} \phi_1 \pm \sin \theta_{4\pm} \phi_5, \quad \psi_{2\pm}^t = \cos \theta_{5\pm} \phi_2 \pm \sin \theta_{5\pm} \phi_6.$$

The difference in the spin polarization of the B  $\pi$  MOs between the singlet and triplet ASDW states is that in the singlet ASDW it is produced by the mixing of the second  $\pi$  LUMO to the second  $\pi$  HOMO and of the third  $\pi$  LUMO to the third  $\pi$  HOMO, while in the triplet ASDW by the mixing of the third  $\pi$  LUMO to the second  $\pi$  HOMO and of the second  $\pi$  LUMO to the third  $\pi$  HOMO as shown in Fig. 8. As a result, the spin polarization of the second  $\pi$  HOMO is larger in the singlet ASDW, while that of the third  $\pi$  HOMO is larger in the triplet ASDW. Because the second  $\pi$  HOMO is spin polarized more easily than the third one, the spin polarization effect in the singlet ASDW

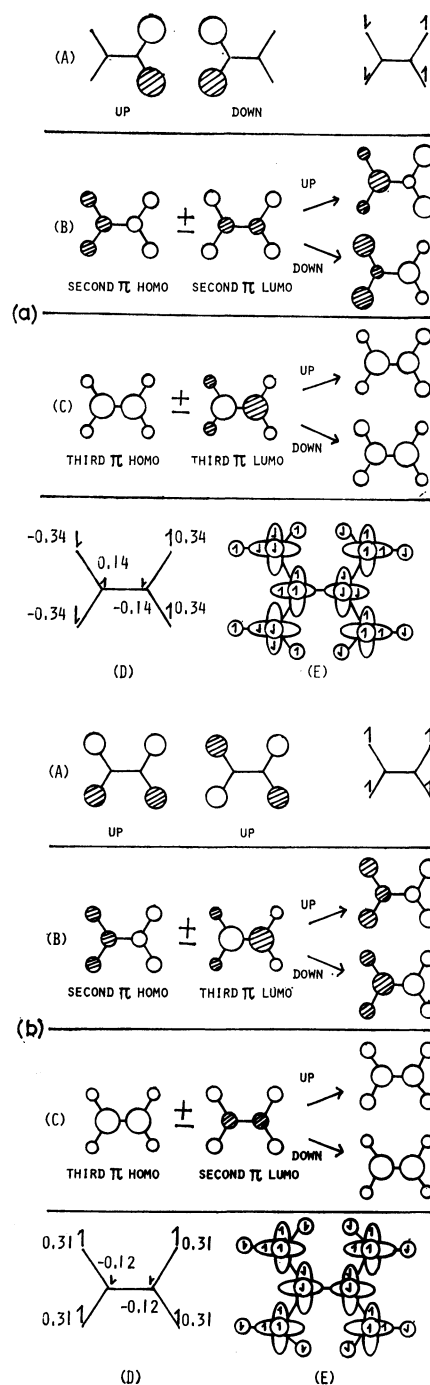


Fig. 8. The corresponding orbitals of the NB  $\pi$  MO (A), second  $\pi$  HOMO (B) and third  $\pi$  HOMO (C) of ASDW1 (a) and the triplet ASDW (b) of tetramethylethane. The spin density structures on the  $\pi$  AOs and  $\sigma$  AOs are also shown in (D) and (E), respectively. The numerals in (D) are the magnitudes of the spin densities. Those on the  $\sigma$  AOs are either  $\pm 0.01$  or  $\pm 0.02$ .

is a little larger than that in the triplet ASDW. This explains why the singlet ASDW lies a little below the triplet ASDW.

The above UHF analysis indicates that the ground state of **3** is singlet and that a triplet state lies close to it. The result is in accord with the *ab initio* CI calcula-

tion by Borden and Davidson.<sup>11)</sup> This suggests that the ESR signal of **3** which was observed at the boiling point of nitrogen<sup>12)</sup> may be attributed to a thermally accessible triplet state. This prediction can be checked by measurement of the temperature dependence of the ESR signal. However, no such experiments have been carried out and the correctness of our prediction is left to be tested.

### Simple Rules to Predict the Spin Multiplicity of the Ground State and the Spin Structure of Low-lying UHF States of Hydrocarbon Diradicals

The above results for **1**, **2**, and **3** show that the UHF theory gives the ground state of correct spin multiplicity. It should be stressed that all the ground states of **1**, **2**, and **3** have alternating spin structures. The results also show that the spin structure of the all-valence-electron UHF calculation is different from that of the two-electron model in such a manner that the weak spin density on an atom adjacent to the atom with large spin density is always antiparallel to the adjacent largest spin density. The preference of the antiparallel spin coupling manifested in the UHF results is consistent with the valence bond picture and seems to have a general validity. By generalizing these results, we can predict the spin multiplicity of the ground state and the spin structure of low-lying UHF states of hydrocarbon diradicals as follows.

Put spins on carbon atoms in alternating directions and if the number of the up and down spins in the alternating spin structure are the same with each other, the ground state is predicted to be singlet, whereas if their difference is two, the ground state is predicted to

be triplet. This rule is much simpler than, but as effective as, the one proposed by Borden and Davidson.<sup>11)</sup> The main aspect of the spin structure of low-lying UHF states is determined by the two-electron model. The all-valence-electron spin structures are obtained by modifying the directions of the weak atomic spin densities so as to make them antiparallel to the adjacent large spin densities.

To demonstrate the general validity of these rules, we apply them to 1,1,2,3,3-pentamethylenepropane (**4**) and 1,3-dimethylenecyclobutadiene (**5**). First we consider **4**. The two NB MOs ( $\phi_A$  and  $\phi_B$ ) obtained with the Hückel Hamiltonian are shown in Fig. 9a. The figure shows that the differential overlap between them is nearly complete, so that there are a singlet ASDW (ASDW1) and a triplet ASDW below the RHF. The spin structures of the NB electrons of the two states are shown in Figs. 9b and 9c. Modifying the weak spin densities so that they are made antiparallel to the adjacent large ones, we obtain Figs. 9b and 9c'. There appear no spin densities on the two central carbons (4 and 5) in Fig. 9b because of the symmetry of the spin structure. The weak spin density on carbon 4 in Fig. 9c' is made negative so as to be antiparallel to the adjacent one. The alternating spin structure corresponds to the triplet state of Fig. 9c', so that the ground state is predicted to be triplet. We show in Fig. 9d the UHF results, which confirm our rules.

Next we consider **5**. The overlap between the two NB MOs ( $\phi_A$  and  $\phi_B$ ) shown in Fig. 10a is medium, so that there are two singlet ASDWs (ASDW1 and ASDW2) and one triplet ASDW below the RHF. The spin structures of the two NB electrons in the three states are shown in Figs. 10b, 10c, and 10d. Modifying the weak spin densities so that they are made antiparallel to

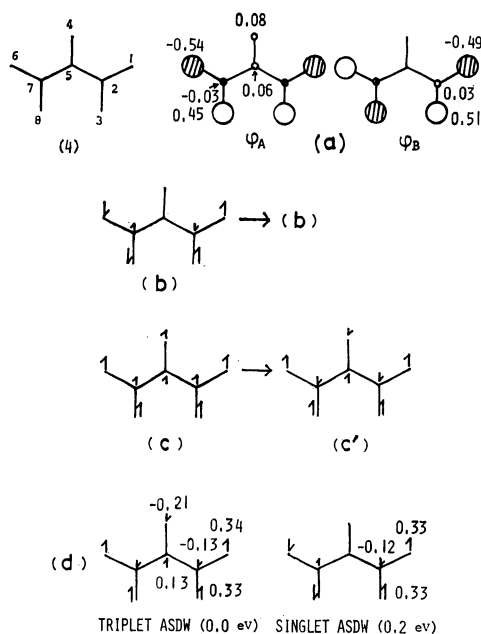


Fig. 9. Two NB MOs (a), the predicted spin structures of ASDW1 (b) and the triplet ASDW (c'), and the result of the all-valence-electron UHF calculation (d) of 1,1,2,3,3-pentamethylenepropane.

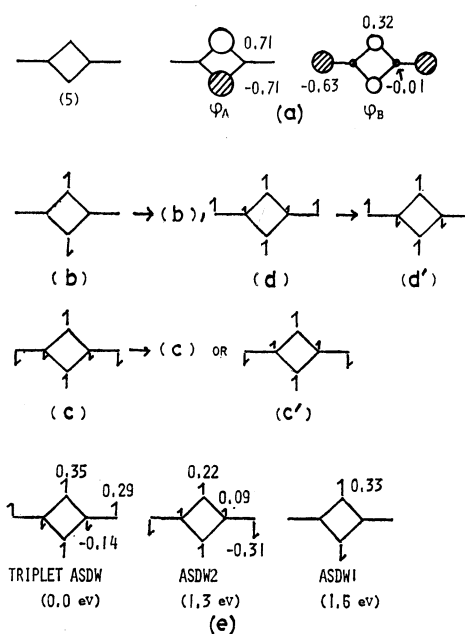


Fig. 10. Two NB MOs (a), the predicted spin structures of ASDW1 (b), ASDW2 (c') and the triplet ASDW (d'), and the result of the all-valence-electron UHF calculation (e) of 1,3-dimethylenecyclobutadiene.

to the adjacent large ones, we obtain the spin structures shown in the right side of Figs. 10b, 10c, and 10d. The spin structure of Fig. 10b is unchanged because of its symmetry. The spin structure of Fig. 10c is possible to be modified in two different ways, but Fig. 10c' shows the feasible one because the terminal carbon atoms have the largest spin densities. The alternating spin structure corresponds to the triplet state in Fig. 10d', so that the ground state is predicted to be triplet. We show in Fig. 10e the UHF results, which also confirm our rules.

#### References

- 1) W. T. Borden, *J. Am. Chem. Soc.*, **97**, 5968 (1975).
- 2) G. Maier, *Angew. Chem. Int. Ed. Engl.*, **13**, 425 (1974); A. Krantz, C. Y. Lin, and M. D. Newton, *J. Am. Chem. Soc.*, **95**, 2744 (1973); O. L. Chapman, C. L. MacIntosh, and J. Pacansky, *ibid.*, **95**, 614 (1973); O. L. Chapman, D. De La Cruz, R. Roth, and J. Pacansky, *ibid.*, **95**, 1337 (1973).
- 3) a) D. R. Yarkony and H. F. Schaefer, III, *J. Am. Chem. Soc.*, **96**, 3754 (1974); b) W. T. Borden, *ibid.*, **97**, 2906 (1975), **98**, 2695 (1976); c) M. J. S. Dewar and J. S. Wasson, *ibid.*, **93**, 3081 (1971); d) J. H. Davis and W. A. Goddard, III, *ibid.*, **99**, 4242 (1977).
- 4) H. Kollmar and V. Staemmler, *J. Am. Chem. Soc.*, **99**, 3583 (1977).
- 5) J. A. Pople, D. L. Beveridge, and P. A. Dobosh, *J. Chem. Phys.*, **47**, 2026 (1967).
- 6) A. Igawa and H. Fukutome, *Prog. Theor. Phys.*, **54**, 1266 (1975).
- 7) H. Fukutome, *Prog. Theor. Phys.*, **52**, 115 (1974); **52**, 1766 (1974).
- 8) P. Dowd, *Acc. Chem. Res.*, **5**, 242 (1972).
- 9) M. Ozaki, *Prog. Theor. Phys.*, **63**, 84 (1980).
- 10) B. G. Odell, R. Hoffmann, and A. Imamura, *J. Chem. Soc., B*, **1970**, 1675.
- 11) W. T. Borden and E. R. Davidson, *J. Am. Chem. Soc.*, **99**, 4587 (1977).
- 12) P. Dowd, *J. Am. Chem. Soc.*, **92**, 1066 (1970).